

## THE HIGHEST DYNAMICAL FREQUENCY IN THE INNER REGION OF AN ACCRETION DISK

M. ALI ALPAR

Faculty of Engineering and Natural Sciences, Sabancı University, Orhanlı, Tuzla, Istanbul 34956, Turkey

AND

DIMITRIOS PSALTIS<sup>1</sup>

Physics and Astronomy Departments, University of Arizona, 1118 E. 4th St., Tucson, AZ 85719

*Draft version July 1, 2019*

### ABSTRACT

In the inner regions of accretion disks around compact objects, the orbital frequency of the gas deviates from the local Keplerian value. For long-wavelength modes in this region, the radial epicyclic frequency  $\kappa$  is higher than the azimuthal frequency  $\Omega$ . This has significant implications for models of the twin kHz QPOs observed in many neutron-star sources that traditionally identify the frequencies of the two kHz QPOs with dynamical frequencies in the accretion disk. The recognition that the highest frequency in the transition or boundary region of the disk is actually the epicyclic frequency also modifies significantly the constraints imposed by the observation of high-frequency QPOs on the mass and radius of the compact objects.

*Subject headings:* accretion disks — waves

### 1. INTRODUCTION

The X-ray brightness of an accreting compact object is often observed to be modulated quasi-periodically at different characteristic frequencies that are comparable to the dynamical timescale of the central object (see, e.g., van der Klis 2005). The physical origin of the various types of quasi-periodic oscillations (QPOs) in accreting black holes and neutron stars are still a matter of debate (see, e.g., Psaltis 2004; van der Klis 2005). Indeed, different variability models attribute the observed QPOs to brightness variations generated at different dynamical frequencies at a particular radius in the accretion disk (e.g., Alpar & Shaham 1985; Miller, Lamb, & Psaltis 1998; Stella, Vietri & Morsink 1999; Abramowicz et al. 2003) or at the frequencies of wave modes in the disk, which are also related to the dynamical frequencies (e.g., Alpar et al. 1992; Alpar & Yılmaz 1997; Wagoner 1999; Kato 2001).

Despite their differences, most proposed models agree that the highest frequency of a large amplitude QPO cannot be larger than the frequency of a stable dynamical oscillation in the accretion disk. Around a non-rotating black hole or a relatively compact neutron star of mass  $M$ , the highest stable dynamical frequency is the azimuthal orbital frequency at the radius of the innermost stable circular orbit

$$f_{\text{ISCO}} = \frac{c^3}{12\pi\sqrt{6GM}}. \quad (1)$$

Requiring this frequency to be larger than the highest observed QPO frequency imposes an upper bound on the mass of the compact object (e.g., Miller, Lamb, & Psaltis 1998) or even provides evidence that the compact object is rapidly spinning (e.g., Strohmayer 2001).

In a realistic accretion disk, the dynamical frequencies of oscillations of fluid elements are approximately equal to the dynamical frequencies of test particles (such as eq. [1]) only away from the boundaries. For example, in the accretion disk around a neutron star with a dynamically important magnetic

field, the orbital frequency of a fluid element near the so-called Alfvén radius (see, e.g., Ghosh & Lamb 1991) deviates significantly from the local Keplerian frequency because of magnetic stresses and viscous stresses (Erkut & Alpar 2005). In accretion flows without large scale magnetic fields, such as those around a non-magnetic neutron star or a black hole, the Maxwell stresses due to turbulent small-scale magnetic fields can also affect the dynamical frequencies in the inner disk (see, e.g., Hawley & Krolik 2001). Even in the absence of any magnetic fields, radiation drag forces can alter significantly the dynamical frequencies at the inner regions of accretion disks (Miller & Lamb 1996).

The magnetic and radiation forces alter the dynamical frequencies predominantly near the inner regions of the Keplerian flows, where the observed QPOs are expected to originate. In this *Letter*, we argue that in realistic accretion disks, in which the azimuthal orbital frequency has a maximum at some radius outside the surface or horizon of a compact object, the radial epicyclic frequency at a comparable radius is the highest dynamical frequency in the system. Our result has significant implications for models of QPOs in accreting compact objects and for the constraints imposed on the masses and spins of the compact objects by the observation of high-frequency QPOs.

### 2. THE HIGHEST DYNAMICAL FREQUENCY

In order to discuss the relative order of different dynamical frequencies in an accretion disk independently of the details of the additional forces that affect the motion of fluid elements, we use the simple but transparent derivation of the equations of motion discussed by Hill (1878). These equations are valid for the motion of test particles in a frame rotating with an angular velocity  $\Omega_0$ , in the presence of additional forces. This set of equations has been used by Balbus & Hawley 1992 to elucidate the physics behind the magnetorotational instability in MHD accretion disks (see also Pessah & Psaltis 2005 for a discussion of a more general case of MHD instabilities).

We start with particles in a stable circular orbit at a radius  $r_0$  and with an angular velocity  $\Omega_0 = \Omega(r_0)$ , i.e.,  $r = r_0$ ,  $\phi = \Omega_0 t$ , where  $\Omega(r)$  is not necessarily the Keplerian angular velocity.

Electronic address: alpar@sabanciuniv.edu  
Electronic address: dpsaltis@physics.arizona.edu

<sup>1</sup> also, Visiting Professor, Sabancı University

Introducing small perturbations around the circular orbit, i.e.,  $r = r_0 + x$  and  $\phi = \Omega_0 t + y/r_0$ , to first order in  $x$  and  $y$ , we obtain the Hill equations

$$\ddot{x} - 2\Omega_0 \dot{y} = -x \left[ r \frac{d\Omega^2}{dr} \right]_0 + f_x \quad (2)$$

$$\ddot{y} + 2\Omega_0 \dot{x} = f_y, \quad (3)$$

where  $f_x$  and  $f_y$  represent the  $x$ - and  $y$ - components of the sum of the perturbations of all forces besides gravity that are acting on the particles. For small displacements away from the stable equilibrium orbit,  $f_x$  and  $f_y$  are linear in  $x$  and  $y$  with negative first derivatives, and hence

$$\begin{aligned} \ddot{x} - 2\Omega_0 \dot{y} &= -x \left[ r \frac{d\Omega^2}{dr} \right]_0 - \left| \frac{\partial f_x}{\partial x} \right|_0 x - \left| \frac{\partial f_x}{\partial y} \right|_0 y \\ \ddot{y} + 2\Omega_0 \dot{x} &= - \left| \frac{\partial f_y}{\partial x} \right|_0 x - \left| \frac{\partial f_y}{\partial y} \right|_0 y. \end{aligned} \quad (4)$$

Looking for solutions of the form  $\sim e^{-i\omega t}$  we obtain the dispersion relation

$$\begin{aligned} \omega^4 - \left( \kappa^2 + \left| \frac{\partial f_x}{\partial x} \right|_0 + \left| \frac{\partial f_y}{\partial y} \right|_0 \right) \omega^2 - 2i\Omega_0 \left( \left| \frac{\partial f_y}{\partial x} \right|_0 - \left| \frac{\partial f_x}{\partial y} \right|_0 \right) \omega \\ + \left( \left[ \frac{d\Omega^2}{d \ln r} \right]_0 + \left| \frac{\partial f_x}{\partial x} \right|_0 \right) \left| \frac{\partial f_y}{\partial y} \right|_0 - \left| \frac{\partial f_y}{\partial x} \right|_0 \left| \frac{\partial f_x}{\partial y} \right|_0 = 0, \end{aligned} \quad (5)$$

where

$$\kappa^2 \equiv 4\Omega_0^2 + \left[ \frac{d\Omega^2}{d \ln r} \right]_0. \quad (6)$$

With axial symmetry,  $\partial f_x / \partial y = \partial f_y / \partial x = 0$ ,

$$\omega^4 - \left( \kappa^2 + \left| \frac{\partial f_x}{\partial x} \right|_0 \right) \omega^2 - 2i\Omega_0 \left| \frac{\partial f_y}{\partial x} \right|_0 \omega = 0. \quad (7)$$

When non-gravitational forces are absent, the solutions are stable modes with  $\omega = 0$  and  $\omega = \kappa$ . As can be verified easily,  $\omega = \kappa$  is the frequency associated with the mode of radial oscillations. As azimuthal perturbations simply shift the phase angle  $\phi$  among equivalent phases on the stable circular orbit ("spontaneous symmetry breaking"), there is no restoring force, and the solution corresponding to azimuthal oscillations is simply  $\omega = 0$ . Indeed, after an azimuthal perturbation the particle would proceed from its shifted phase on the same circular orbit, at the original orbital frequency  $\Omega_0$ . This is an instance of the Goldstone theorem that zero frequency modes are associated with spontaneous symmetry breaking. The physical reason for the nonzero restoring force and nonzero frequency  $\omega = \kappa$  for radial perturbations is rotation. The long range correlations introduced by the presence of rotation, i.e., the Coriolis force and the gradient of the centrifugal potential provide the restoring force in the Hill equations (4). Modes effected by long range forces always have nonzero frequencies, as exemplified by the plasma frequency due to the Coulomb force, the Jeans mass associated with gravitational instabilities, and the finite mass of Higgs bosons.

The effect of short-range forces can be traced in the realistic limit

$$\left| \frac{\partial f_x}{\partial x} \right|_0, \left| \frac{\partial f_x}{\partial y} \right|_0, \left| \frac{\partial f_y}{\partial x} \right|_0, \left| \frac{\partial f_y}{\partial y} \right|_0 \ll \kappa^2. \quad (8)$$

The  $\omega \simeq \kappa$  modes are now quasi-stable with  $\mathcal{R}(\omega) \simeq \kappa$  and  $\mathcal{I}(\omega) \sim \mathcal{O}(|\partial f_{x,y}/\partial x|_0/\kappa) \ll \mathcal{R}(\omega)$ . There is still an exact  $\omega = 0$  mode, due to the axial symmetry and a decaying mode with

$\mathcal{R}(\omega) = 0$  and  $\mathcal{I}(\omega) \sim -\mathcal{O}(\kappa)$ . This decay corresponds to the effect of the shear on the initial perturbations.

When the disk is treated as a continuous medium and its hydrodynamic or magnetohydrodynamic wave modes are studied, the analogues of restoring forces on perturbations of single particle orbits in the Hill equations are spatial derivatives of the forces on a fluid element. These restoring force terms contain the product  $(\vec{V}_A \cdot \vec{k})^2$  or  $(c_s k)^2$  where  $\vec{k}$  is the wave vector, and  $\vec{V}_A$  and  $c_s$  are the Alfvén velocity and sound speed respectively (see, e.g., Alpar et al. 1992; Balbus & Hawley 1992; Alpar & Yılmaz 1997; Kato 2001; Pessah & Psaltis 2005). Conditions analogous to (8) describe global modes of long wavelength. These modes are expected to be the ones that produce the largest amplitude of brightness modulation. In the limit of small wavenumber  $k$ , the frequencies of oscillations have values close to  $\kappa$  and  $\Omega$ . For modes with  $m$  azimuthal nodes, frequencies comparable to  $\kappa - m\Omega$  will appear; the dominant global modes will be those with  $m = 0$  and  $m = 1$ , which represents the beat between the radial epicyclic frequency and the disk rotation. This fundamental effect of rotation can be seen in all dispersion relations of waves in rotating fluids and accretion disks, in models of varying degrees of complexity (see, e.g., Chandrasekhar 1961; Papaloizou & Pringle 1984). We emphasize here that not all oscillations described by the Hill equations are stable. This is of particular relevance to MHD disks that are subject to the magnetorotational instability, especially at the limit of small wavenumbers.

Where magnetic or radiation forces significantly affect the orbital motion of gas elements, the azimuthal frequency in the disk differs from the local Keplerian value. As an example, for accretion onto a rotating and magnetic neutron star, the local azimuthal frequency  $\Omega(r)$  is lower than the Keplerian frequency inside some characteristic radius  $r_2$  comparable to the Alfvén radius. It has a maximum  $\Omega_{\max}$  at  $\bar{r} < r_2$  and then decreases to match the rotation frequency of the star  $\Omega_*$  at a radius  $r_1$ , which marks the disk-magnetosphere boundary. The simplest mathematical model employs a quadratic form for  $\Omega(r)$ ,

$$\Omega(r) = \begin{cases} \Omega_{\max} - (\Omega_{\max} - \Omega_*) \left( \frac{r - \bar{r}}{r_1 - \bar{r}} \right)^2, & r \leq r_2 \\ (GM/r^3)^{1/2}, & r > r_2 \end{cases}, \quad (9)$$

where  $M$  is the mass of the star. Matching these two expressions, as well as their derivatives, at  $r_2$  relates the maximum frequency and its location to the transition region parameters  $r_1$ ,  $r_2$ ; and the neutron-star rotation rate  $\Omega_*$ :

$$\Omega_{\max} = \frac{\Omega_*/\Omega_2 - (9/16)(r_1/r_2 - 7/3)^2}{\Omega_*/\Omega_2 + (3/2)(r_1/r_2 - 5/3)} \Omega_2 = \frac{7}{4} \left( 1 - \frac{3}{7} \frac{\bar{r}}{r_2} \right) \Omega_2. \quad (10)$$

This model quite accurately represents the  $\Omega(r)$  curves that meet a boundary condition at the stellar magnetosphere and asymptotically join the Keplerian curve within a transition region in models of accreting neutron stars with dynamically important magnetic fields Erkut & Alpar 2005. The model of the azimuthal frequency profile described by equation (9) is shown in Figure 1, for  $\Omega_2/\Omega_* = 1.1$ ,  $\Omega_{\max}/\Omega_* = 1.2$ , and  $r_1/r_2 = 0.84$ , together with the radial epicyclic frequency calculated according to equation (6).

At radii  $r < r_2$ , where the azimuthal frequency is lower than the Keplerian frequency, the radial epicyclic frequency is the larger of the two dynamical frequencies. At the radius  $\bar{r}$ , where the azimuthal frequency has a maximum,  $\kappa = 2\Omega_{\max}$

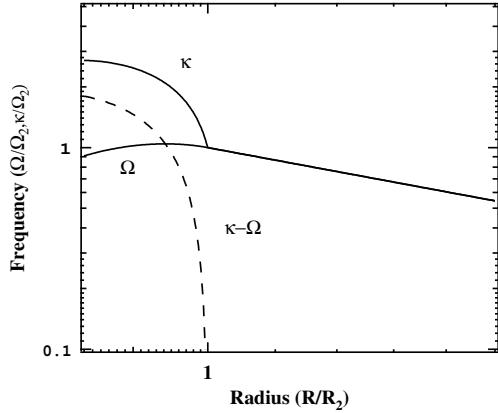


FIG. 1.— The radial profile of the azimuthal ( $\Omega$ ) and radial epicyclic ( $\kappa$ ) frequencies of the simple model discussed in the text, for  $\Omega_*/\Omega_2 = 1.1$  and  $r_1/r_2 = 0.4$ . The dashed line shows the difference  $\kappa - \Omega$ . At radii  $r > r_2$  the azimuthal and radial epicyclic frequencies are equal to the Keplerian frequency.

and the ratio  $\kappa/\Omega$  increases to even larger values in the region  $r_1 < r < \bar{r}$ , where the azimuthal frequency is decreasing with decreasing radius. For a wide range of radii inside  $r_2$ , the radial epicyclic frequency is larger than the local Keplerian frequency. As a result, if low- $k$  modes in this transition region are responsible for the observed QPOs in accreting neutron stars and black holes, as envisioned by most models, then an upper bound of the QPO frequencies may be set not by the maximum azimuthal frequency but by the maximum radial epicyclic frequency in the region.

### 3. DISCUSSION

In §2, we argued that, in the inner regions of accretion disks around compact objects, magnetic, radiation, pressure, and viscous forces may become comparable to the gravitational force, alter the orbital frequencies of fluid elements and lead to radial epicyclic frequencies in excess of the orbital frequencies. Here, we discuss the implications of our results for models of the kHz QPOs observed from many accreting neutron-star sources (for a review see van der Klis 2005). These are pairs of QPOs with frequencies comparable to a kHz that vary on timescales longer than any of the dynamical timescales in the vicinity of the neutron stars.

As the frequencies of the kHz QPOs vary, they follow a number of intriguing patterns. In all sources for which the spin frequency of the neutron star is known, either via observations of X-ray pulses or burst oscillations, the difference frequency between the two kHz QPOs was shown to be comparable to the neutron star spin frequency or to half its value. This property gave rise to the beat-frequency models of kHz QPOs (see Strohmayer et al. 1996; Miller et al. 1998; Chakrabarty et al. 2003). In sources for which the frequencies of the two kHz QPOs were measured with high accuracy, such as Sco X-1, it was shown that the two frequencies followed a quadratic correlation (Psaltis et al. 1998; Psaltis, Belloni, & van der Klis 1999). Together with the correlation between the frequencies of the kHz QPOs and other low-frequency QPOs observed simultaneously in the same sources, this provided support for the relativistic precession models (Stella & Vietri 1999; Stella, Vietri, & Morsink 1999; Psaltis & Norman 2000). Finally, the ratios of the frequencies of the two kHz QPOs are roughly comparable to the ratio  $2/3$  and this

gave rise to models that rely on resonances between modes (Abramowicz et al. 2003). It is important to note here that, mathematically speaking, not all three of the above patterns can characterize simultaneously the frequency correlations of the kHz QPOs and, in fact, none of them is valid to within the measurement errors of the QPO frequencies. However, all three of them can be shown to be able to describe the data roughly, typically to within 30% for the first and last alternative and to within 5% for the quadratic correlation (see Psaltis et al. 1998 for a detailed discussion of the statistical significance of various correlations).

In all the models of the kHz QPOs mentioned above, one or both of the observed QPO frequencies are interpreted as dynamical frequencies (azimuthal, radial, or vertical) at different characteristic radii in the accretion flows. For each of these models, these dynamical frequencies have been calculated so far assuming that the only force that affects the motion of fluid elements is gravity, even though there is always an implicit assumption that some additional physical mechanism picks the characteristic radius where these QPOs originate. As we have shown, the relative ordering of the frequencies for long-wavelength modes depends on the radial profile of the azimuthal frequency. Therefore, the identification of observed QPOs with particular dynamical frequencies may not be self consistent in any of the above models.

For most realistic models of the azimuthal frequency, e.g., for the quadratic model discussed in §2 (eq. [9]), the largest of the dynamical frequencies is  $\kappa$  and the smallest is  $\Omega$ , in the inner part of the transition region where  $d\Omega/dr > 0$  (see also Fig. 1). Wavepackets in the disk can modulate the accretion flow onto the compact object at the radial epicyclic frequency band  $\sim \kappa$ , at the orbital frequency band  $\sim \Omega$ , or at the beat  $\kappa - \Omega$  of the radial and orbital motions. It is clear that  $\kappa \geq 2\Omega$  and therefore  $\kappa - \Omega \geq \Omega$  in the region  $d\Omega/dr > 0$ , where the order of the frequencies is  $\kappa > \kappa - \Omega \geq \Omega$ .

How does one identify the observed upper and lower kHz QPO frequencies, hereafter  $\nu_2$  and  $\nu_1$ , respectively, with two of these three possible frequencies? There are two simple trends that all kHz QPOs are observed to obey: (i) the two kHz QPO frequencies always increase or decrease together, and (ii) their difference  $\Delta\nu \equiv \nu_2 - \nu_1$  decreases as both frequencies increase. The only pair of frequencies that satisfies these two conditions are  $\kappa$  and  $\kappa - \Omega$ . Indeed, if we associate these two frequencies with the upper and lower kilohertz QPO frequencies, i.e.,  $\kappa = 2\pi\nu_2$  and  $\kappa - \Omega = 2\pi\nu_1$ , they will satisfy the trend (ii) if  $d\Omega/d\kappa < 0$ , which is equivalent to

$$\frac{d \log(\Omega d\Omega/dr)}{d \log r} < -5. \quad (11)$$

This condition holds as long as the transition region size is about a fifth of the disk inner radius or less.

Perhaps the most interesting application of kilohertz QPO models is the constraints they provide on the mass-radius relation of neutron stars (Miller et al. 1998; see also discussion after Eq. [1]). The interpretation of the highest QPO frequency as the epicyclic rather than the Keplerian azimuthal frequency modifies the bounds obtained from the upper kilohertz frequency. To estimate the effect of the phenomena discussed here on the bounds in the mass-radius plane, we use the simple model (9). In this model, the maximum epicyclic frequency, to a first approximation, is equal to the radial epicyclic frequency at radius  $\bar{r}$  and hence

$$2\pi\nu_{2,\max} \simeq \kappa(\bar{r}) = 2\Omega_{\max}. \quad (12)$$

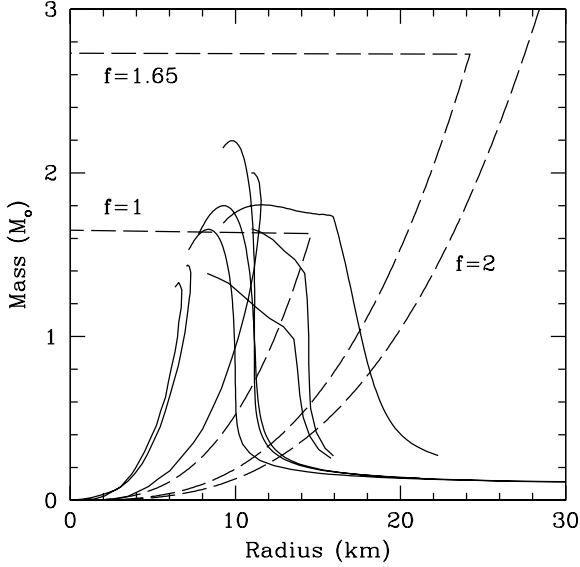


FIG. 2.— Constraints on the mass-radius plane of neutron stars imposed by the observation of the highest frequency QPO so far (1330 Hz, see van Straaten et al. 2000) for different values of the parameter  $f$  (see, eq. [14]). The solid lines show the predictions of representative equations of state for neutron-star matter (see Lattimer & Prakash 2001).

The constraints the kHz QPOs impose on the mass and the radius of a neutron star are obtained from two requirements. First, the neutron star radius  $r_{\text{NS}}$  must be less than a representative inner disk radius that is associated with upper kilohertz QPO frequency, which was interpreted as a Keplerian frequency in earlier applications (see van der Klis 2005). Recognition of the epicyclic frequency as the highest frequency modifies this constraint to

$$r_{\text{NS}} < \frac{(GM)^{1/3}}{(2\pi\nu_2)^{2/3}} f^{2/3}, \quad (13)$$

where the factor

$$f \equiv \left[ \frac{\kappa(\bar{r})}{\Omega_K(\bar{r})} \right] \simeq \frac{7}{2} \left( \frac{\bar{r}}{r_2} \right)^{3/2} \left( 1 - \frac{3\bar{r}}{7r_2} \right) \quad (14)$$

depends on the width of the transition region. The second constraint simply states that the radius of the last stable orbit is less than the disk radius associated with the upper kilohertz QPO,  $r_{\text{ISCO}} = 6GM/c^2 < \bar{r}$ . This leads to

$$M < \left( \frac{c^3}{6\sqrt{6}G} \right) \frac{f}{2\pi\nu_2}, \quad (15)$$

if the upper kilohertz QPO is the radial epicyclic frequency rather than the Keplerian frequency. For an infinitely narrow boundary layer,  $f = 2$ , while for  $\bar{r}/r_2 = 0.9$  and  $0.8$ ,  $f = 1.84$  and  $1.65$  respectively. The resulting modified constraints are shown in Figure 2. We conclude that a careful interpretation of the kHz QPO frequencies makes the constraints on the masses and radii of neutron stars much less stringent.

We note that in general relativity, the radial epicyclic frequency for test particle orbits deviates from the Keplerian form at radii close to  $r_{\text{ISCO}}$ . Unlike the Newtonian case, in general relativity, radial and vertical epicyclic frequencies do not coincide with the azimuthal frequency. Simple derivations of epicyclic oscillation frequencies in the (Newtonian, as well as) general relativistic cases are provided by Abramowicz & Kluzniak (2004), who give expressions for the dynamical frequencies in terms of the metric. General relativistic expressions for the radial epicyclic frequency incorporating fluid effects and appropriate formulations of the metric around the neutron star will be the subject of future work. By continuity from the Newtonian treatment here, we anticipate that the highest frequency will turn out to be the radial epicyclic frequency at radii  $r_1, \bar{r} > r_{\text{ISCO}}$  by factors of a few.

M. A. A. thanks the Physics Department of the University of Arizona, D. P. thanks Sabancı University, and both authors thank the University of Amsterdam for hospitality during the writing of this paper. M. A. A. acknowledges support from the Turkish Academy of Sciences and the Sabancı University Astrophysics and Space Forum. D. P. acknowledges support from the NASA grant NAG-513374.

#### REFERENCES

- Abramowicz, M. A., Karas, V., Kluzniak, W., Lee, W. H., & Rebusco, P. 2003, *PASJ*, 55, 467
- Abramowicz, M. A., & Kluzniak, W. 2004, in *From X-ray Binaries to Quasars: Black Hole Accretion on All Mass Scales*, astro-ph/0411709
- Alpar, M.A., Hasinger, G., Shaham, J. and Yancopoulos, S. 1992, *A&A*, 257, 627
- Alpar, M.A. and Shaham, J. 1985, *Nature*, 316, 239
- Alpar, M.A. and Yilmaz, A. 1997, *New Astronomy*, 2, 225
- Balbus, S.A. and Hawley, J.F. 1992, *ApJ*, 392, 662
- Chakrabarty, D., Morgan, E. H., Muno, M. P., Galloway, D. K., Wijnands, R., van der Klis, M., & Markwardt, C. B. 2003, *Nature*, 424, 42
- Chandrasekhar S. 1961, *Hydrodynamic and Hydromagnetic Stability*, Clarendon, Oxford, pp. 589-591.
- Erkut, M.H. and Alpar, M.A. 2005, *ApJ*,
- Ghosh, P., & Lamb, F. K. 1991, *NATO ASIC Proc. 344: Neutron Stars*, 363
- Hawley, J. F., & Krolik, J. H. 2001, *ApJ*, 548, 348
- Hill, G.W. 1878, *Am.J.Math.*, 1, 5
- Kato, S. 2001, *PASJ*, 53, 1
- Lattimer, J. M., & Prakash, M. 2001, *ApJ*, 550, 426
- Miller, M. C., & Lamb, F. K. 1996, *ApJ*, 470, 1033
- Miller, M. C., Lamb, F. K., & Psaltis, D. 1998, *ApJ*, 508, 791
- Papaloizou, J.C.B. and Pringle, J.E. 1984, *MNRAS*, 208, 721
- Pessah, M. and Psaltis, D. 2005, *ApJ*, 628, 879
- Psaltis, D. 2004, *AIP Conf. Proc. 714: X-ray Timing 2003: Rossi and Beyond*, 714, 29
- Psaltis, D., Mendez, M., Wijnands, R., Homan, J., Jonker, P.G., van der Klis, M., Lamb, F.K., Kuulkers, E., van Paradijs, J. and Lewin, W.H.G. 1998, *ApJ*, 501, L95
- Psaltis, D., et al. 1998, *ApJ*, 501, L95
- Psaltis, D., Belloni, T., & van der Klis, M. 1999, *ApJ*, 520, 262
- Psaltis, D., & Norman, C. 1999, astro-ph/0001391
- Stella, L. and Vietri, M. 1999, *Phys. Rev. Lett.*, 82, 17
- Stella, L., Vietri, M., & Morsink, S. M. 1999, *ApJ*, 524, L63
- Strohmayer, T. E. 2001, *ApJ*, 552, L49
- Strohmayer, T. E., Zhang, W., Swank, J. H., Smale, A., Titarchuk, L., Day, C., & Lee, U. 1996, *ApJ*, 469, L9
- Wagoner, R. W. 1999, *Phys. Rep.*, 311, 259
- van der Klis, M. 2005, in *Compact Stellar X-ray Sources*, (Cambridge: University Press), astro-ph/0410551
- van Straaten, S., Ford, E. C., van der Klis, M., Méndez, M., & Kaaret, P. 2000, *ApJ*, 540, 1049